Technical Report

In support of data uploaded for DE EE0007603
"Assessing rare earth element concentrations in geothermal and oil and gas produced waters: A potential domestic source of strategic mineral commodities"

Description: This report contains rare earth element, geochemical, and isotope concentrations of water produced alongside oil and gas operations in Wyoming.

Project PI: S.A. Quillinan[1]

Contributing Authors: C. Nye[1], S.A. Quillinan[1] G. Neupane[2], and T. McLing[2],

[1] University of Wyoming, Laramie Wyoming
[2] Idaho National Laboratory, Idaho Falls, Idaho

Executive Summary:

This study is a joint effort by the University of Wyoming (UW), the UW Engineering Department (UW-ENG), and Idaho National Laboratories (INL) and the United States Geological Survey to describe rare earth element concentrations in oil and gas produced waters. In this work we present the Rare Earth Element (REE) and trace metal character of produced water in several oil and gas fields and three coal fired power stations. power stations.
The concentration of Rare Earth Elements (REEs) in oil and gas produced waters is largely unknown. For example, of the 150,000 entries in the USGS National Produced Waters Geochemical Database less than 5 include data for REEs. Part of the reason for this deficit is the analytical challenge of measuring REEs in high salinity, hydrocarbon-bearing waters. The leading industry standard for water analysis struggles to detect REEs in natural waters under ideal conditions. In the complex samples of oil and gas fields, where background noise and interferences are worsened by the high concentrations of non-REE ions and residual hydrocarbons, the detection of REEs becomes even more challenging. INL project team members continue to refine and develop these methodologies throughout the course of this work. Using the methods of the INL team members we were able document REEs in high salinity oil and gas waters for the first time.

Preliminary results show that REEs exist as a dissolved species in all waters measured for this project, typically within the part per trillion range. Data are provided within this report along with a description of analytical method development.

Sample Inventory:

The Wyoming Oil and Gas Thermal Water (OGTW) samples were collected new for this project, and will be combined with previously collected samples from USGS team members. OGTW samples were given extra attention so that they could form a robust training set for the Emergent Self-Organizing Map (ESOM) that we plan to produce. This attention included duplicate analyses from internal and external labs and matching to an analogous rock sample. The rock-water sample matches are shown in Figure 1 and described in the sister report for the rock portion of this project.The Wyoming sample set reported here contains 43 oil and gas thermal waters, and 11 industrial thermal waters.

The OGTWs have sample name prefixes MD, PRB, LC, WA, LB, and MS. The OGTWs split into two significant sub-types, those taken on a well-pad before mixing, and those taken after mixing either with other wells in a gather station or atmospheric air in a holding tank. The main difference in these sub-types is the temperature of the water. As such, the recorded temperatures shown in Appendix B should be considered minimums, with the true well-head temperature being higher. Two samples, MD-7 and LC-31, were collected after passing through a flash-tank to remove H_2S and consequently record lower temperatures. The pH of OGTWs is weakly basic to weakly acidic and shows great variety in conductivity. The Oxidation-Reduction Potential (ORP) was recorded in some samples when the meter was available and not at risk of hydrocarbon fouling. The ORP in the highest hydrocarbon samples tends to be positive (LB-48), and in deep wells negative (such as LB-42).

The industrial thermal waters have prefixes DJPP, WYDAK, LR, and JBPP. These samples show the changes that occur during cooling. The good constraints on the sequence allow many variables to be controlled. They are weakly basic to very basic, but not very conductive. JBPP-32 was not collected by the investigators so few field parameters are available for it.

Formation	Water	Rock
Almond	WA-34 WA-36 WA-37 WA-39	T932-10340 T932-10342 T932-10350 T932-10359 T932-10344
Cody	MS-58 MS-59 MD-2 MD-4	C899 D031 C233-8790.5 C233-8615.5
Fort Union	MD-7	S462-7416 S462-7428 S462-7431
Fort Union-Lance	MD-8	C233-8615.5 C233-11919.5
Frontier	PRB-18 PRB-19	E173-12218 E173-12224 E173-12230 E173-12232 E173-12227.5
	LB-46 LB-47	B209-6676 B209-6175 B209-6189 B209-6697 B209-6708 B209-6185
Frontier/Baxter	LB-43 LB-45	B209-6676 B209-6185 D904-4558 D904-4568 D904-4582 D904-4541.5 D904-4547 D904-4553.5
Lance	MS-53 MS-54 MS-56	S716 S755
Lewis-Almond	WA-33 WA-35 WA-38 WA-40	T932-10340 T932-10344 T932-10323 T932-10294 T932-10342 T932-10350 T932-10359
Lower Fort Union	MS-51 MS-52 MS-57	S716 S755
Maddison	LB-42	D037-7499 D037-7496 D037-7504 D037-7536 D037-7538 D037-7593 D037-7581
Madison-Basement	LC-31	GA00018 24785-24800 GA00018 24700-24715 GA00018 23505-23520
Madison	LC-31	D380-2058 D380-2060 D380-2061
Mesa-Verde	MS-50	C899 D031
Mowry	PRB-15	W075-10646.5 W075-10657.5 W075-10663 W075-10650
Muddy	LB-44 LB-48	D839-8217 D839-8195 D839-8192.5 D839-8200 D839-8204 D839-8210
Niobrara	PRB-10	A648-6143 A648-6136.5 A648-6143 A648-6146 A648-6140
	PRB-16	W074-1198 E815-9182 E815-9133 E815-9140 E815-9164 E815-9190 E815-9199 E815-9202 E815-9218
Parkman	PRB-12 PRB-14	A029-7321.5 A029-7299.85 A029-7310.5 A029-7317
Shannon	PRB-17	E183-10616 E183-10624.5 E183-10647 E183-10643.5
Turner	PRB-11 PRB-13	E124-10108.5 E124-10113 E124-10116 E124-1025 E124-10135.5
Upper Fort Union	MD-3	S462-7416 S462-7428 S462-7431

Figure 1: A table of the Wyoming geologic formations sampled for this project. This table lists the sample codes for water, and the Core Research Center (CRC) codes for rock. The samples are grouped to show which rock sample(s) matches which water sample(s).

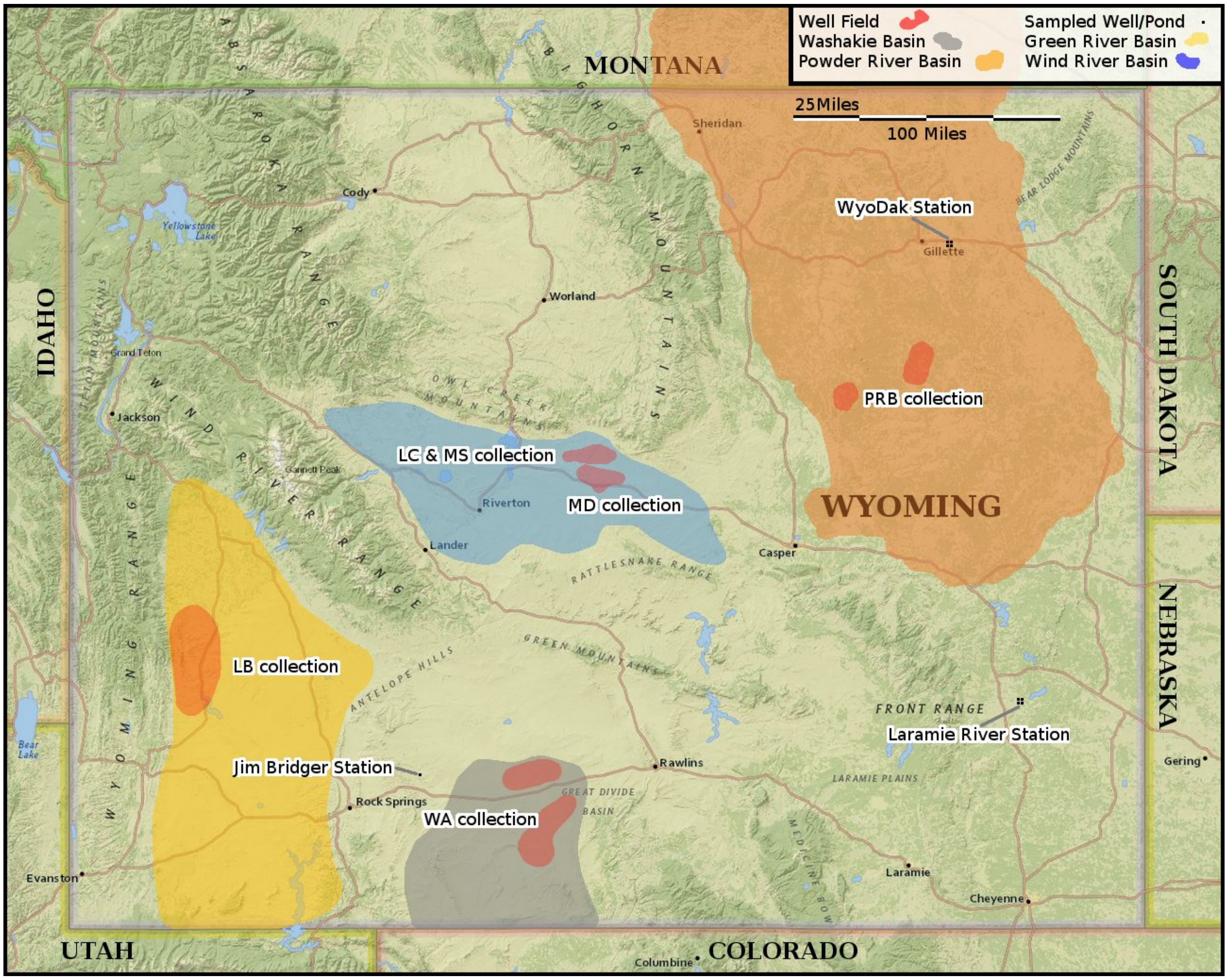

Figure 2: The Wyoming OGTW sample locations are shown on this map in red. The four regions and their sample prefixes are also shown. Note the three different prefixes for the Wind River Basin.

Methodology:

Sample Collection, Preparation, and Transport Methods:

Samples were collected in three or four 500ml bottles at each site. Processing and all analysis is possible with 1.5L but if the coolers had extra space, 2L were sometimes collected. All bottles were washed, and rinsed with sample prior to final collection and sealing. Once per collection day, a field blank was collected. These blanks used 1.5L of nanopure DI-water from the CMI laboratory, which was poured into the 500ml bottles in the field, during a random one of the first six sampling stops of that collection trip. After sealing, the field blank bottles were treated exactly like all other samples from that collection.

Bottles were labeled at the collection point with a two letter abbreviation for their region and a unique number that indicates the well or well-gather-station. All bottles were stored on blue gel-ice during transport. Upon return to Laramie, the bottles were frozen overnight to halt bacterial growth. This reduces fractionation of carbon isotopes, and preserves the original ratio of microbe species.

In CMI's laboratory, within 48 hours of collection, the three or four bottles for each site were poured into a filter-funnel and filtered under vacuum with 0.45µm millipore mixed cellulose ester filter-papers. This produced an average blend of the three or four bottles, and removed suspended solids. While filtering would often remove heavy hydrocarbons, light hydrocarbons (such as gas condensate) would pass the filter.

Analysis	Acidified	Volume	External
Anion Geochemistry	No	50mL	No
Anion Geochemistry	No	50mL	Yes
Cation Geochemistry	Yes	15mL	No
Cation Geochemistry	Yes	15mL	Yes
Isotopes (C, O, H)	No	30mL	No
Isotopes (Sr, O, H)	No	50mL	Yes
REE (aqueous)	Yes	500mL	No (INL)
Backup reserve	No	~500mL	No
Meta-genomics	No	Filter Papers	Yes

Figure 3: Summary of sample aliquots. The filtered sample was split into nine aliquots. For those aliquots that were acidified trace metal grade nitric acid was used. All samples were stored in a

refrigerator until analysis. If transported to INL or an external lab, they were shipped on blue gel-ice.

INL's REE Measurement Methods

OGTWs are susceptible to all three of the traditional barriers to REE quantification in natural waters with the current industry standard of ICP-MS. First, sample salinity, especially barium concentrations, causes a fluctuating baseline and also direct carrier-gas mass interferences that are so computationally difficult to back-out it is functionally infeasible. Second, hydrocarbons entrained with the sample can foul the delicate instrumentation, and introduce mass interferences in the same way as salinity. Third, the low concentration of REEs in natural waters is only just within the detection range of ICP-MS, resulting in non-detection with even slight miscalibration, and masking from even the smallest source of contamination. The following method overcomes each of these three traditional obstacles.

We used two sample processing/pre-concentration protocols- one for samples with relatively low (TDS= 4500 mg/L) total dissolved solids (TDS) and the other for samples having TDS up to 300 g/L. Figure 4 shows the general flow charts of our low and high TDS pre-concentration protocols. In short, the low-TDS sample pre-concentration protocol uses AG-50W- X8 hydrogen form resin in the 200 mesh to 400 mesh size. Previous studies (e.g., Elderfield and Greaves 1982; Klinkhammer et al. 1994; Johannesson et al. 2011; McLing et al. 2014) reported that this size fraction results in a lower flow rate through the column and increases the REE capture efficiency.

The samples were processed to concentrate the REE by continuous gravity feeding of sample through a resin containing chromatography column (20 mL Bio-Rad column) with a 250-mL sample reservoir. For this method, the amount of resin used varies based on the cation makeup and total TDS of the water as follows: AG-50W- X8 (mL) = 0.0038 × TDS (mg/L) (for 500 mL of Ca-Mg rich waters) AG-50W- X8 (mL) = 0.0046 × TDS (mg/L) (for 500 ml of Na rich waters) For some very-low TDS water, the calculated volume of AG-50W- X8 can be as little as 1 or 2 mL. This allows very rapid flow of water through the column; in such cases, we use 5 mL of AG 50W-X8 to increase sample residence time in the column. For a given volume of water, TDS, and major cations, the volume of AG-50W- X8 ranges from 5 to 20 mL (20 mL is the maximum volume our columns can hold). If the calculated amount of AG- 50W-X8 needed is more than 20 mL, we use the protocol developed for high TDS samples based on a different resin (described below). After the sample chromatography was completed, the eluent was discarded. Optima nitric acid (2.5 M) eight-times greater than the resin volume is then added to the reservoir to elute divalent cations from the resin, leaving behind only the trivalent cations retained in the resin. The REE and other trivalent cations are then eluted from the resin using four times the resin volume of higher-strength Optima nitric acid (8 M) and collected in an acid-washed Teflon container.

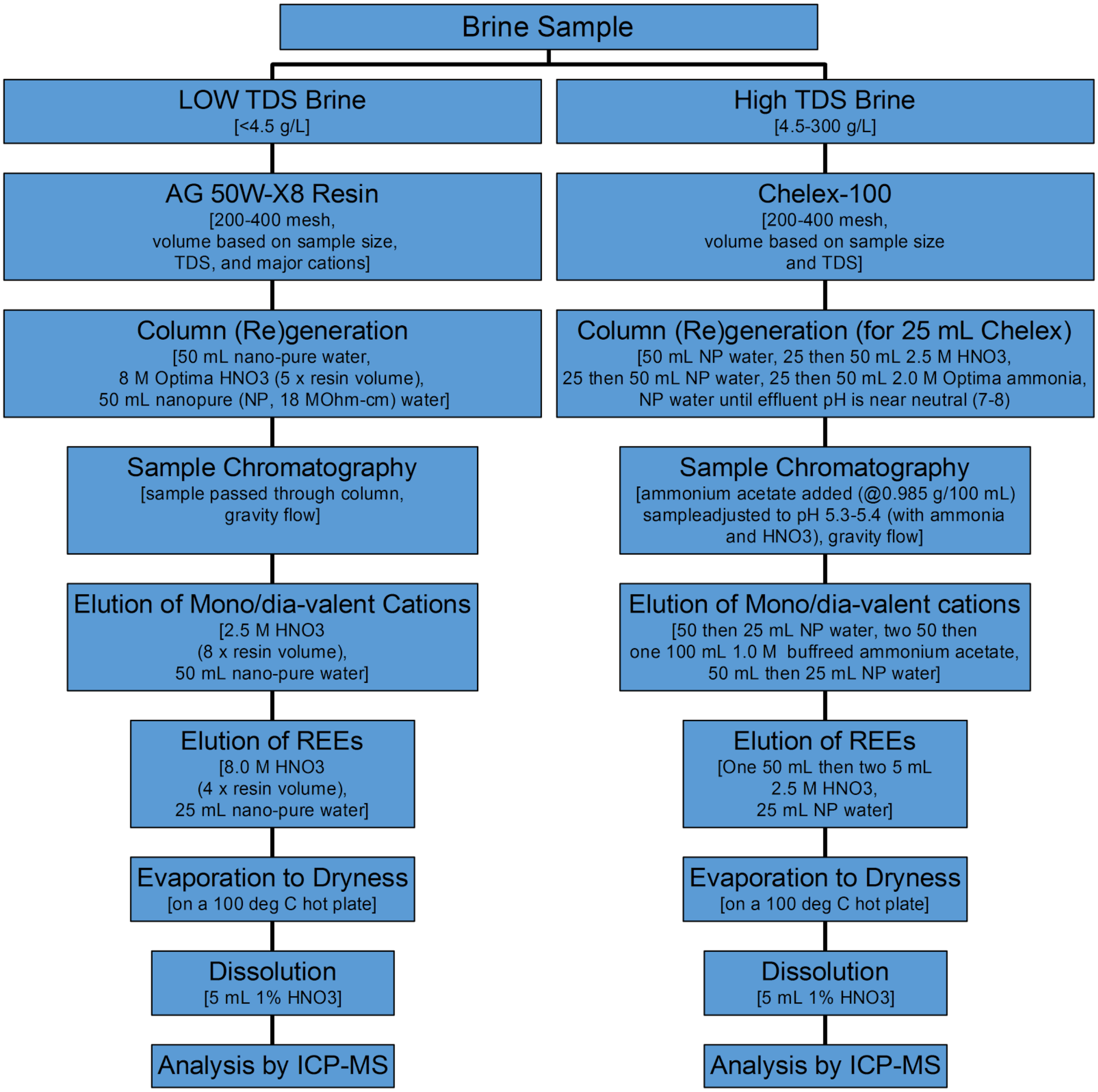

Figure 4. Flowcharts of INL pre-concentration protocols low- and high-TDS aqueous samples for REE analysis (NP water: nano-pure, de-ionized water). For high-TDS samples, a modified method based on Strachan et al. (1989) was used to concentrate the REE from solution. This procedure uses 200–400-mesh Chelex 100 resin in the Na form.

In summary, each column containing 16.25 g of resin was flushed with 75 mL of 2.5 M Optima nitric acid to convert the resin to hydrogen form and remove any non-hydrogen cations. The initial acid wash was followed by a 50-mL DIW water wash to remove excess nitric acid from the resin. Then the resin was converted to NH_4^+ form by passing 60 mL of 2.0 M of high-purity ammonium hydroxide solution, which was followed by DIW water washes to a neutral pH. The sample is treated with ammonium acetate (0.985/100 mL) then adjusted to 5.3±0.1 using Optima nitric acid/ammonium hydroxide solution to attain the optimal pH of 5.3 for the best cation capture.

Once the resin was prepared, the REE in each sample were nominally concentrated by 50:1 or 100:1 by gravity-feeding nominally 500 mL or 1,000 mL of sample through the column, first adding two 50-mL aliquots of sample to allow the resin volume to shrink without forming preferential flowpaths. Once the entire sample was passed through the column, 3-5 batches of 25-50 mL DIW water was applied. The column was then eluted with a few batches of 25-50 mL of pH-adjusted (pH = 5.3±0.1) 1.0 M high-purity ammonium acetate to remove the mono- and divalent cations. Then the REE is eluted with 2.5 N Optima nitric acid after rinsing with a few batches of DIW (Figure 4). The final REE extract obtained with both low- and high-TDS procedures was evaporated to dryness at about 100°C on a hot plate enclosed in a filter box to eliminate contamination by dust. The resulting bead was then dissolved in a 10-mL 1% Optima nitric acid to obtain the final concentration ratio of approximately 50:1 or 100:1. The sample was then sealed in a triple acid-washed, 15-mL centrifuge tube for ICP-MS analysis.

Method development addressed the concern that reduced pre-concentration ratios would cause the signal of some REEs would disappear into background noise during analysis, resulting in a non-detect. Study of the tolerances of the Agilent 7900 ICP-MS during analysis suggested that if the concentration of REEs in the initial sample were comparable, samples as small as 100mL should still be detectable and statistically distinct from noise. This calculation gave the team confidence that a high-REE sample as small as 100mL could be extracted and analyzed. Successful analysis of the five such samples under the High-TDS method confirmed this prediction.

Part of INL's original intent when developing the REE method was to eventually make it possible for others to implement this method with typical industry instrumentation. To stretch the present method below 30ml will almost certainly require a next-gen ICP-MS such as the Agilent 8900 triple quadrapole just released. Switching to this instrument would put the present method beyond the reach of typical industry instrumentation and much of the scientific community. However, in sample-limited cases switching to a next-gen instrument could make REE analysis possible.

Geochemistry:

Data Tables

Anions, Cations, and Trace element chemistry are listed in Appendices C and D.

Narative

Geochemistry analysis was performed for standard anions and cations, as well as selected trace elements at both internal and external labs. Both internal and external labs measured anions by Ion Chromatography (IC) and cations by Inductively Coupled Plasma - Optical Emission Spectrometry (ICP-OES). Trace elements were analyzed at the same time as cations. The in-house instruments used were the dual-channel Dionex ICS 500 IC for anions and the Perkin Elmer Optima 8300 ICP-OES for cations and trace elements.

The water types are generally consistent within basins. Sodium is the major cation in every sample, with calcium being significant in some less briney samples. Chloride, carbonate and sulfate make up the majority of anions in all waters. Significant chloride occurs in all OGTWs. Many also contain significant carbonate, which in the case of MD samples surpasses even the chloride concentration. Industrial thermal waters are unique in their high sulfate concentrations which dwarf both chloride and carbonate. Minor anions tend to follow the trend of a major anion such as bromide following chloride.

Trace elements are variable. Barium, Silicon, and Strontium are most common but vary wildly even within the same field and basin. In industrial waters, some elements like Aluminum concentrate in the lower ponds, while others like Lithium and Boron have the greatest concentration factors in the ponds experiencing the greatest evaporation.

Rare Earth Elements:

Data Tables

REE ratios when normalized to North Pacific Deep Water are listed in Appendix E and pre-normalization in Appendix F.

Data Table Narrative

In most OGTWs LREE are enriched over HREEs, with a significant positive Eu anomaly. While this distinctive behavior is best seen on the spider diagrams below, the data tables also show this trend. The formula for LREE to HREE enrichment in each sample is:

$$\mathbf{La_{NPDW} / Yb_{NPDW}} = \textbf{the light to heavy enrichment factor}$$

And the formula for the Eu anomaly in each sample is:

$$\mathbf{Eu / Eu^* = Eu_{NPDW} / (Sm_{NPDW} \times Gd_{NPDW})^{-½}} = \textbf{the Eu anomaly}$$

The normalized La is greater than normalized Yb in all except six samples, showing that LREEs are enriched over HREEs. Also, the normalized Eu is greater than its neighbors Sm and Gd in all samples except one, showing that aqueous Eu is present in greater concentrations than one would expect based on its neighbor elements.

In pre-normalized concentrations often La then Ce are the most abundant REEs in water. These are often followed by Eu then Nd then Yb. Present sources of La and Ce are bountiful, and of very low economic value. However, Eu, Nd, and Yb are in high demand, and of high economic value.

Spider Diagrams

The following Spider Diagrams show the relative concentration of REEs among samples. These plots are a common convention in REE research. These plots use normalization to North Pacific Deep Water (NPDW), which is the most common normalization for water. NPDW is defined as:

REE	ng/L (ppt)
La	5.375817
Ce	0.5576776
Pr	0.718641
Nd	3.432912
Sm	0.6781236
Eu	0.1884304
Gd	1.0740175

REE	ng/L (ppt)
Tb	0.1795909
Dy	1.36175
Ho	0.3859362
Er	1.3280444
Tm	0.2077839
Yb	1.512457
Lu	0.2554562

Figure 5: The North Pacific Deep Water Normalization as reported by Alibo and Nozaki, 1999. These values were converted to ng/L from pico-mol/kg to match the conventions of this project. The second column, containing the heavy REEs, shows the alternating high-low concentration predicted by the Oddo–Harkins rule. The rule holds for the light REEs too, but it is less apparent due to Promethium's radioactive decay and the ocean's depletion in Cerium.

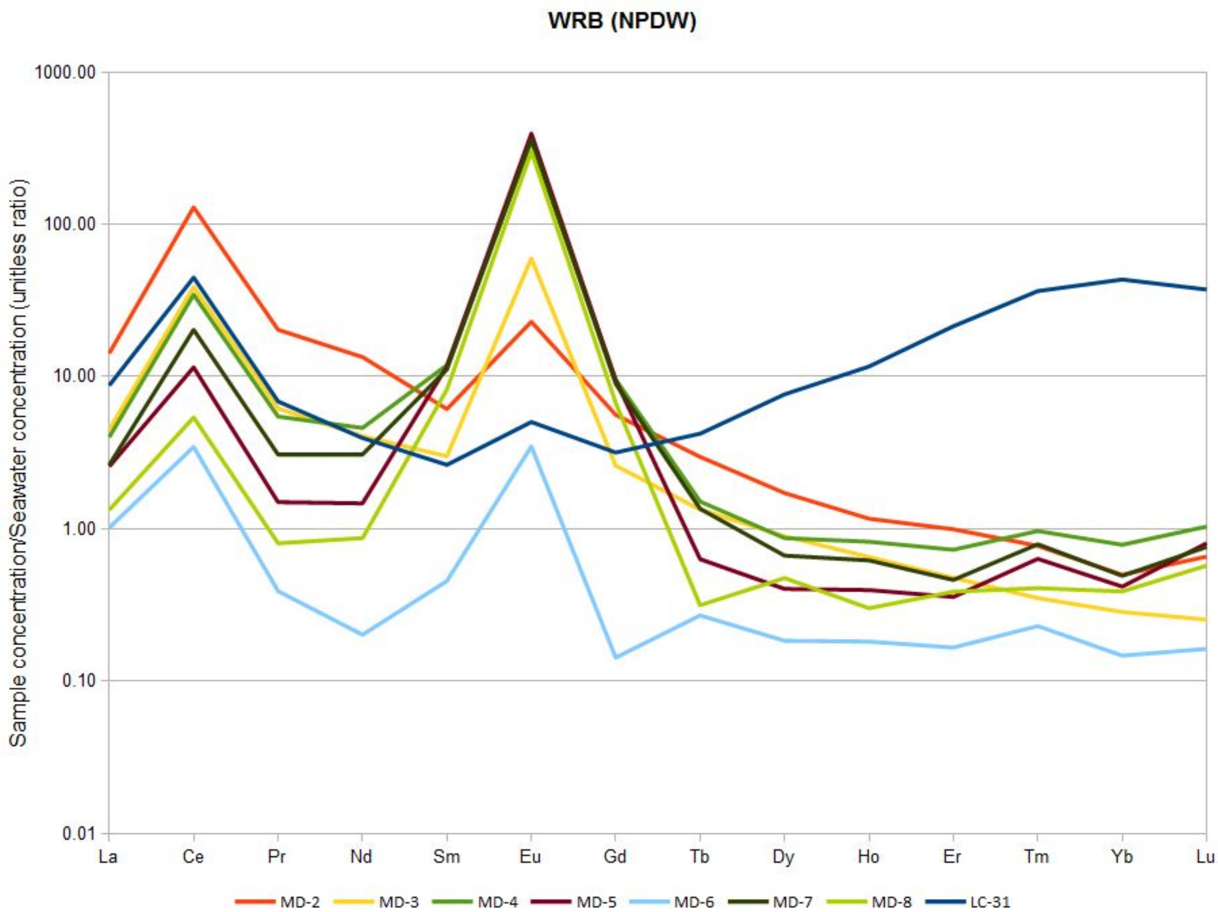

Figure 6a: Spider diagram of the REEs in Moneta Divide and Lost Cabin OGTWs. All OGTWs have a europium positive anomaly. However, the LC-31 sample which samples water from the Madison limestone has a smaller anomaly. Europium is most often hosted in calcium-minerals, such as those found in limestone. LC-31 also exhibits the only HREE over LREE enrichment in this set. MD-6 is the concentrated reject brine that comes out of a reverse-osmosis water treatment plant. Its uniform depletion relative to the input water (MD-5) suggests that REEs either build-up in some part of the water treatment plant or that they remain in the purified water.

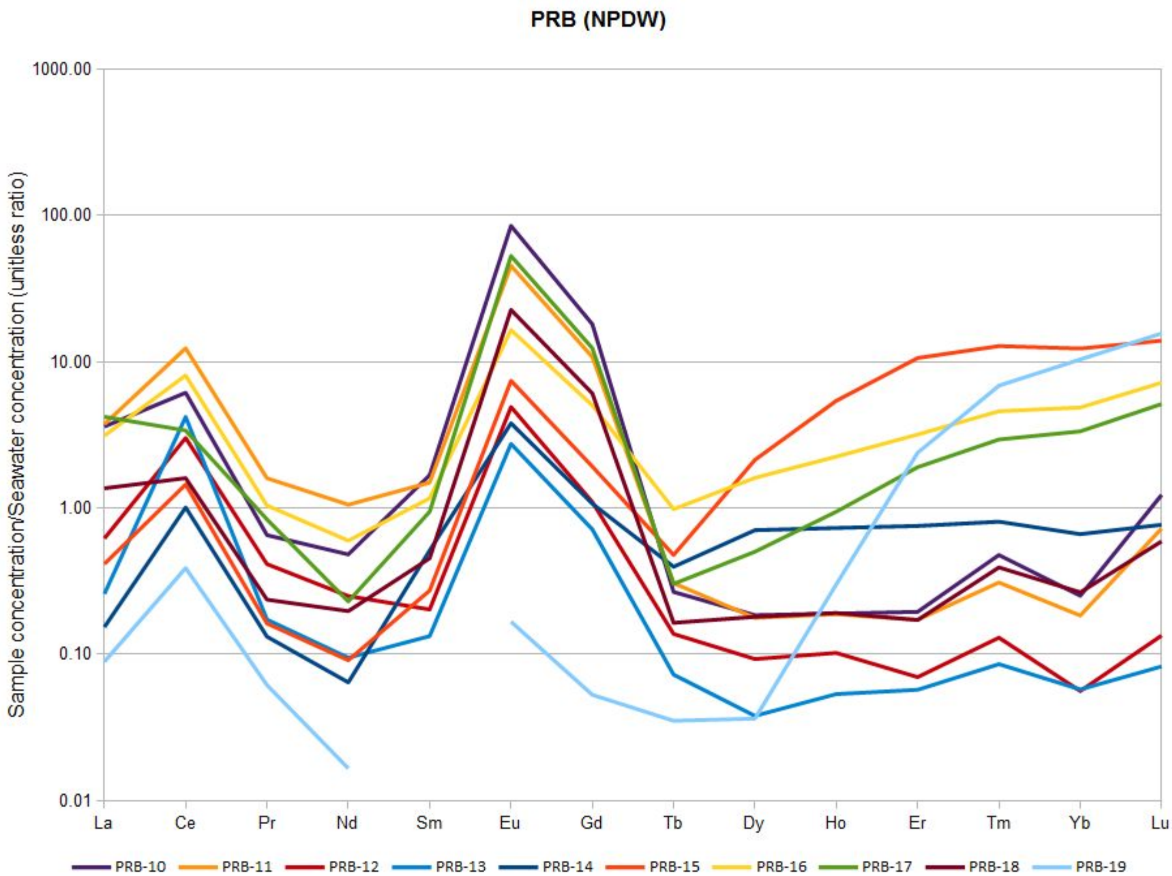

Figure 6b: Spider diagram of the REEs in Powder River Basin OGTWs. The PRB is unique because it has a positive gadolinium anomaly nearly as strong as the Europium anomaly. Some samples also show HREE over LREE enrichment, although this is not consistent for all wells in the basin. The gap in PRB-19 is a result of samarium being below the detection limits of our method in that one sample.

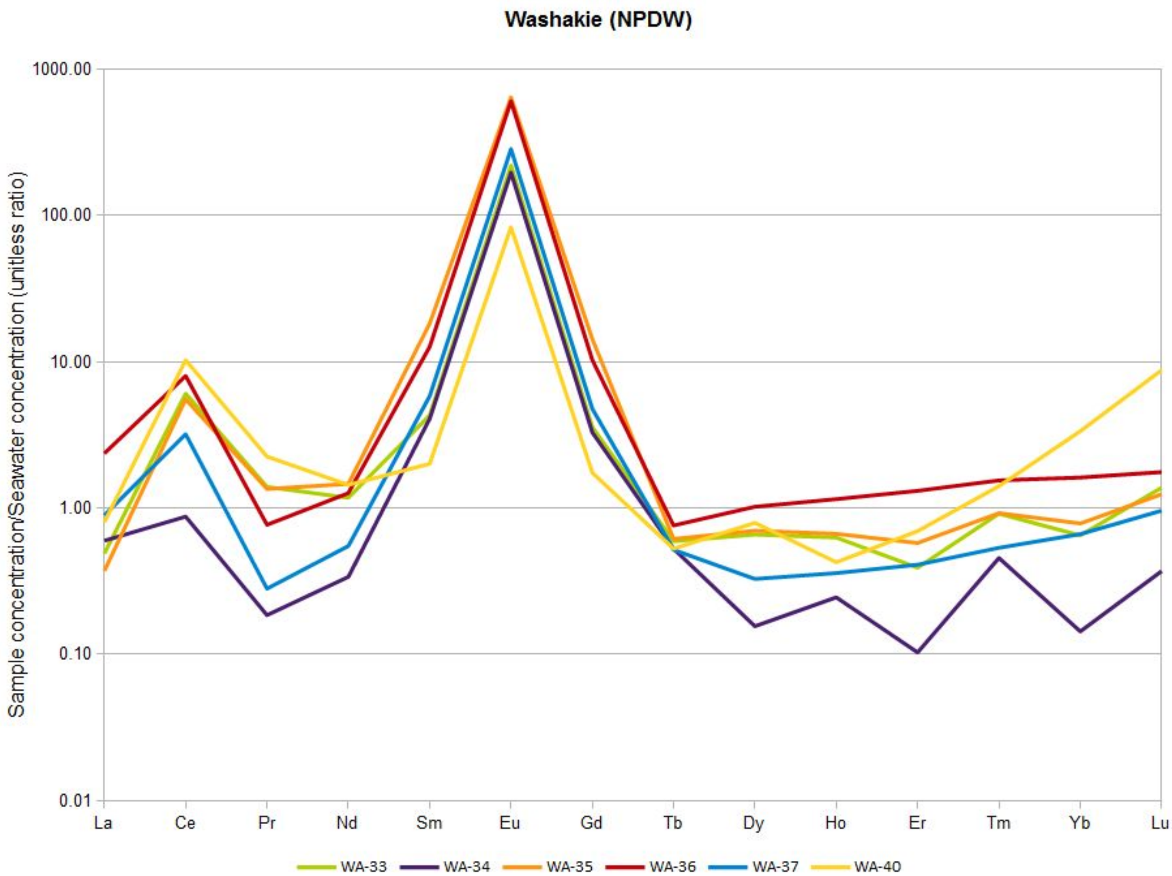

Figure 6c: Spider diagram of the REEs in OGTWs from the Wamsutter area of the Washakie basin. Some sample numbers such as WA-38 and WA-39 were unprocessable due to their high concentrations of soap and other additives. Aside from these all other samples in the area show consistent REE patterns. Samples from this area have flat LREE/HREE enrichments and an "A"-type enrichment of the middle REEs; samarium, europium, and gadolinium.

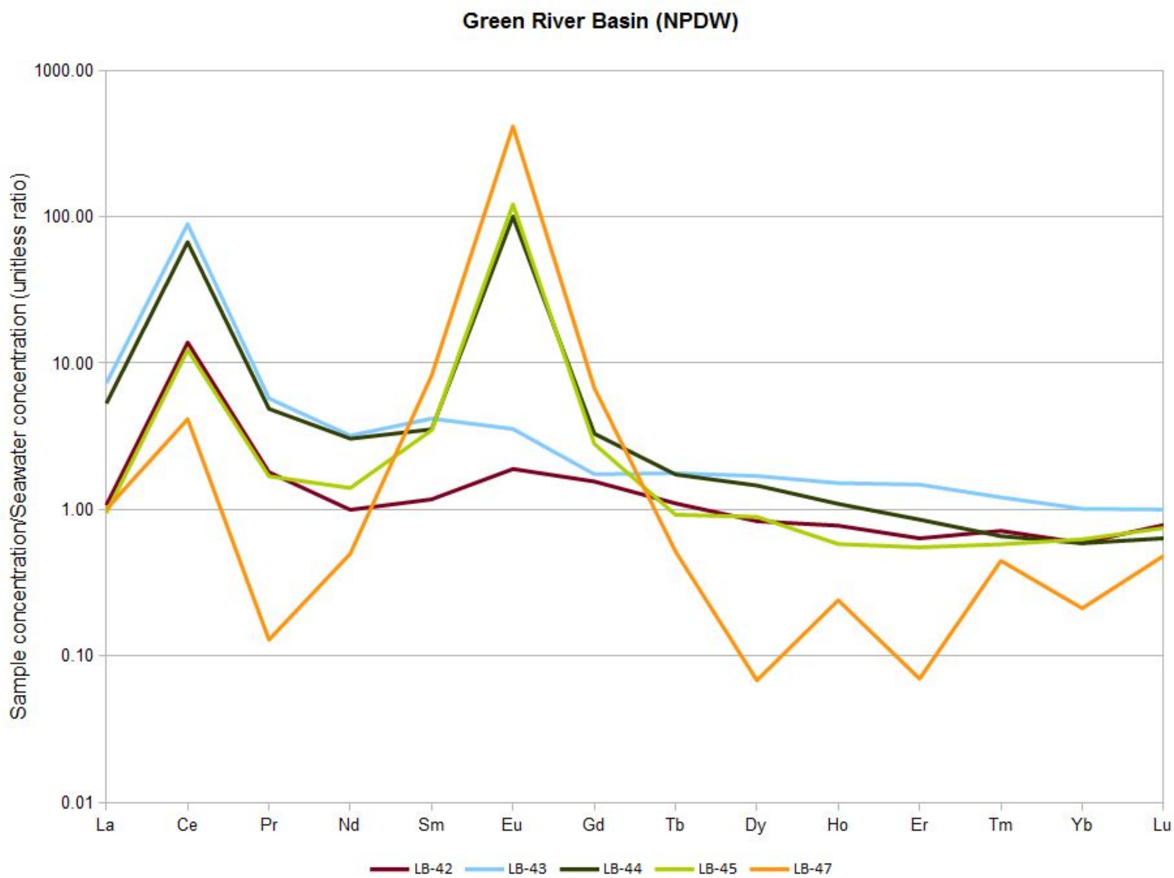

Figure 6d: Spider diagram of the REEs in Green River Basin OGTWs. Sample LB-42 came from the Madison limestone, just as LC-31 did, although the samples are in different basins. They both show a comparatively very small positive europium anomaly. This suggests that the chemistry for the madison limestone, or some other factor which does not differ between basins, causes only a small amount of europium to enter the water. Gaps in this dataset, such as LB-46, were a result of collecting condensate with little or water..

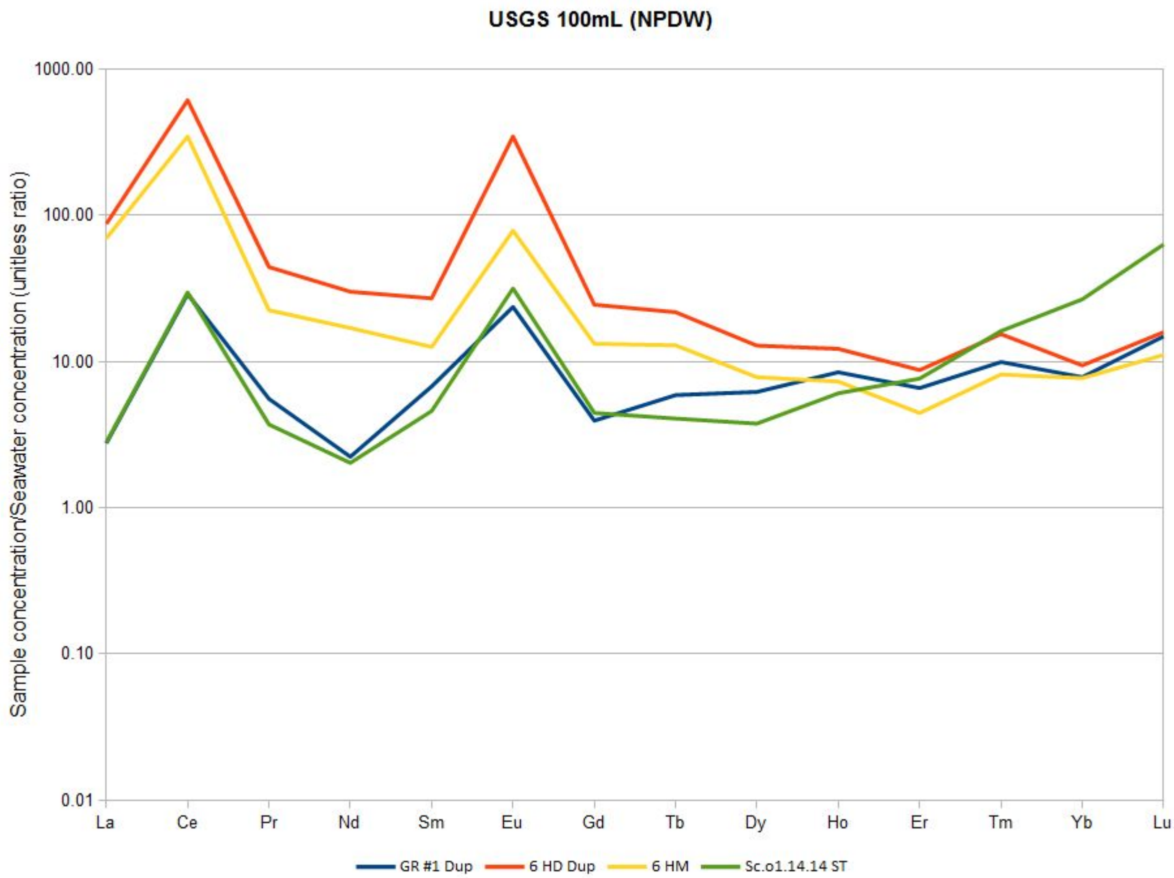

Figure 6e: Spider diagram of the REEs in OGTWs from the USGS library. These deep basin brines have consistent enrichment patterns, and in absolute terms the greatest concentration of REEs sampled. These waters contain roughly ten times more REEs than the ocean.

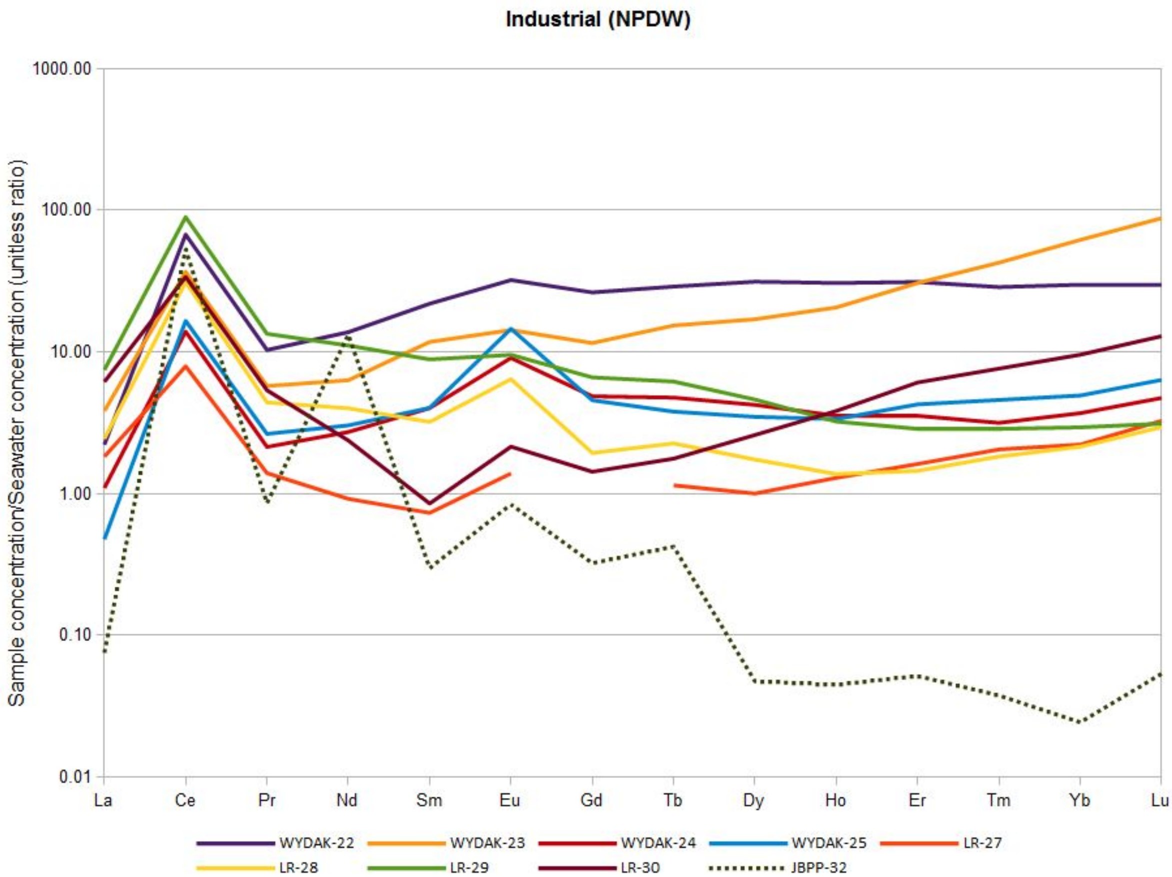

Figure 6f: Spider diagram of the REEs in industrial power station ash ponds. These surficial samples lack the Europium anomaly found in other samples, having at most very small positive anomalies. The samples have generally higher HREEs than the OGTWs. JBPP-32 was the only sample not collected in-person for this study and of questionable quality as seen in the even-odd trend apparent even after normalization.

<u>Spider Diagram Narration</u>

Because the ocean loses much of its dissolved Ce due to a well understood and naturally occurring reduction-oxidation reaction any water that does not undergo a similar reaction will be comparatively enriched in Ce. As Ce is one of the most common and least valuable REEs this anomaly should be ignored.

Although most OGTW spider diagrams exhibit the same pattern, some are noticeably shifted toward greater concentrations. For example, the relative proportions of each REE in PRB-10 and PRB-12 are similar (as seen in the similar shape of their lines) yet PRB-10 is over twice as concentrated as PRB-12 in absolute terms (as seen in its upward shift on the y-axis). It is important to consider both the relative proportions of REE and their absolute concentrations displayed on a spider diagram.

The other important observation revealed by spider diagrams is that HREEs in the PRB vary greatly in concentration from one sample to the next, even if less than 25 miles apart in the same formation. This high variability is not seen in the MD samples from the Wind River Basin, in the LB samples from the Green River Basin, nor in the WA samples from the Washakie Basin.
This signature is most visible in the PRB samples and WA samples. The PRB signature is a Gd positive anomaly to nearly the level of Eu. The WA signature is a flat LREE:HREE ratio with "A"-type enrichment of the MREEs.

Isotopes:

Data Tables

Stable isotope ratios normalized to VSMOW and VPDB are listed in Appendix G.

Narrative

Isotopes of δD and $\delta^{18}O$ of water

Isotopes of water were measured for all newly collected samples (Figure 7, Appendix G). With the exception of one sample all plot below the global meteoric water line. Relative to water rocks have an enriched oxygen isotope ratio, waters that exhibit an enriched $\delta^{18}O$ signature--like the waters measured in this study-- indicate interaction with host rocks. An interaction such as this is permissive evidence for REE between water and rock.

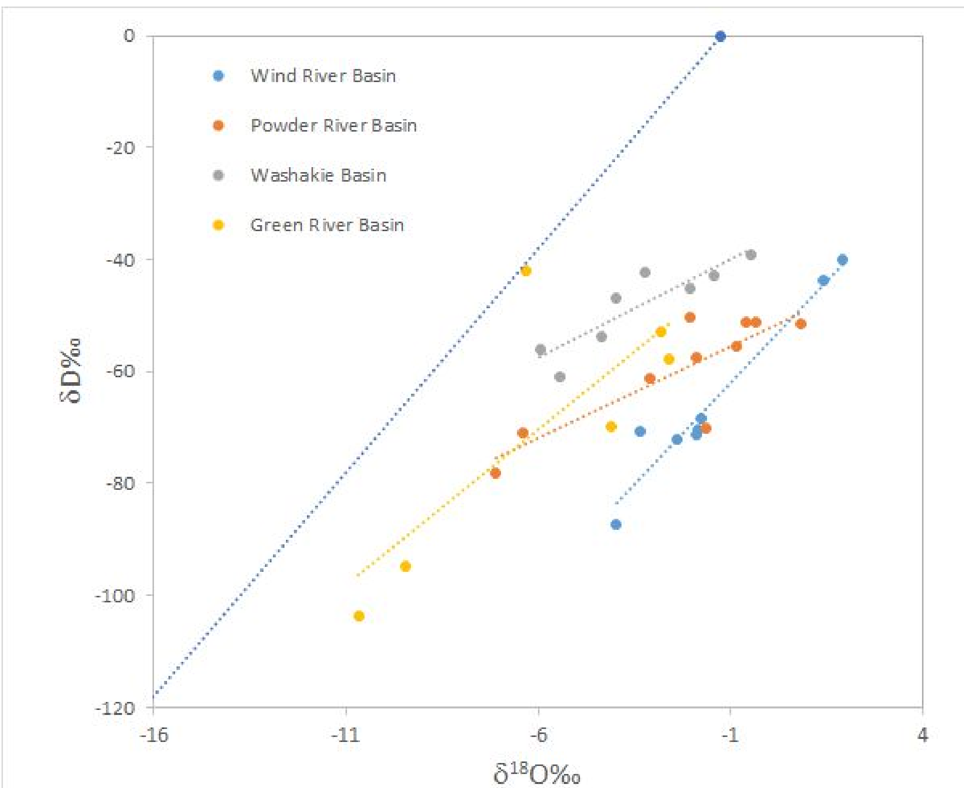

Figure 7: Oxygen and Deuterium stable isotopes on a standard D-O plot normalized to Vienna Standard Mean Ocean Water (VSMOW). All points lie to the right of the Global Meteoric Water Line (GMWL) in dark blue. High temperature, long duration interaction with host rocks normally causes samples to plot in this region. Points further from the GMWL have likely experienced a longer or stronger interaction than those close to the GMWL.

Carbon isotopes

Carbon isotopes were measured in geologic basins known to have biogenic methane, the Wind River Basin and Powder River Basin. The processes that produce biogenic methane isotopically fractionate Dissolved Inorganic Carbon (DIC). Studies have used this diagnostic DIC isotope signature of water associated with biogenic gas generation to trace produced water on the surface (Quillinan and Frost, 2013) and in the subsurface (Martini, 1998; Sharma and Frost, 2008; McLaughlin et al., 2011; Quillinan and Frost, 2012). For this study we found that only the Wind River basin was influenced by biogenic gas. Illustrated in Figure 8 we show the carbon isotope ratios normalized to Vienna Pee Dee Belemnite (VPDB) as a function of the bicarbonate concentrations. Note the linear correlation between $\delta^{13}C_{DIC}$ and HCO_3 mg/L in the Wind River Basin. Although some of the Powder River Basin samples show elevated $\delta^{13}C_{DIC}$ the absence of an elevated concentration of HCO_3 indicate they are not associated with biogenic methanogenesis. During further interpretation we will consider this variable for the Wind River Basin as it pertains to rare earth element concentrations of waters in natural gas reservoirs.

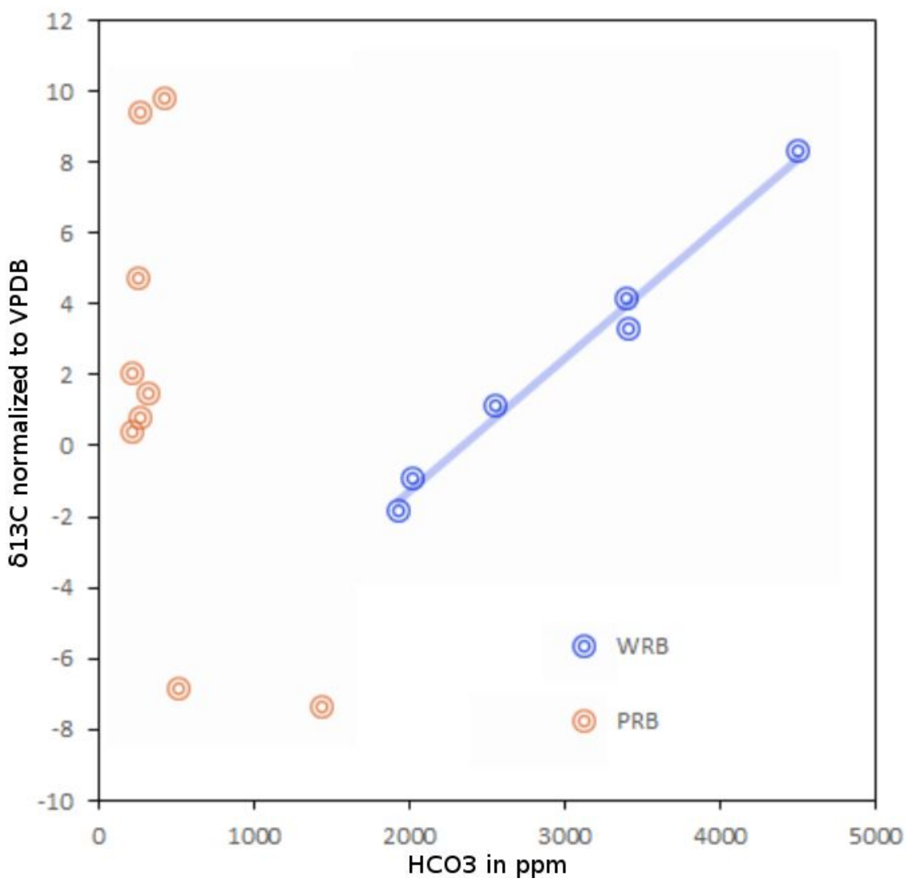

Figure 8: The linear relationship of δ^{13}CDIC to HCO_3 concentration is evidence for biogenic methane production in the WRB samples.

Strontium Isotopes

Strontium isotope ratios were measured for 22 samples. Strontium is a divalent cation and readily substitutes for calcium in carbonates, sulfates, and feldspars. The ratio of 87/86 strontium has an accuracy to six significant figures and can be a strong indicator of water-rock interaction and the origin of salinity. Strontium isotopes in this study ranged from 0.70842 to 0.73457, indicating a wide range of continental weathering and sediment types. They form distinct groups matching the basins and formations they sample. This confirms we were successful in sampling various geologic terrains.

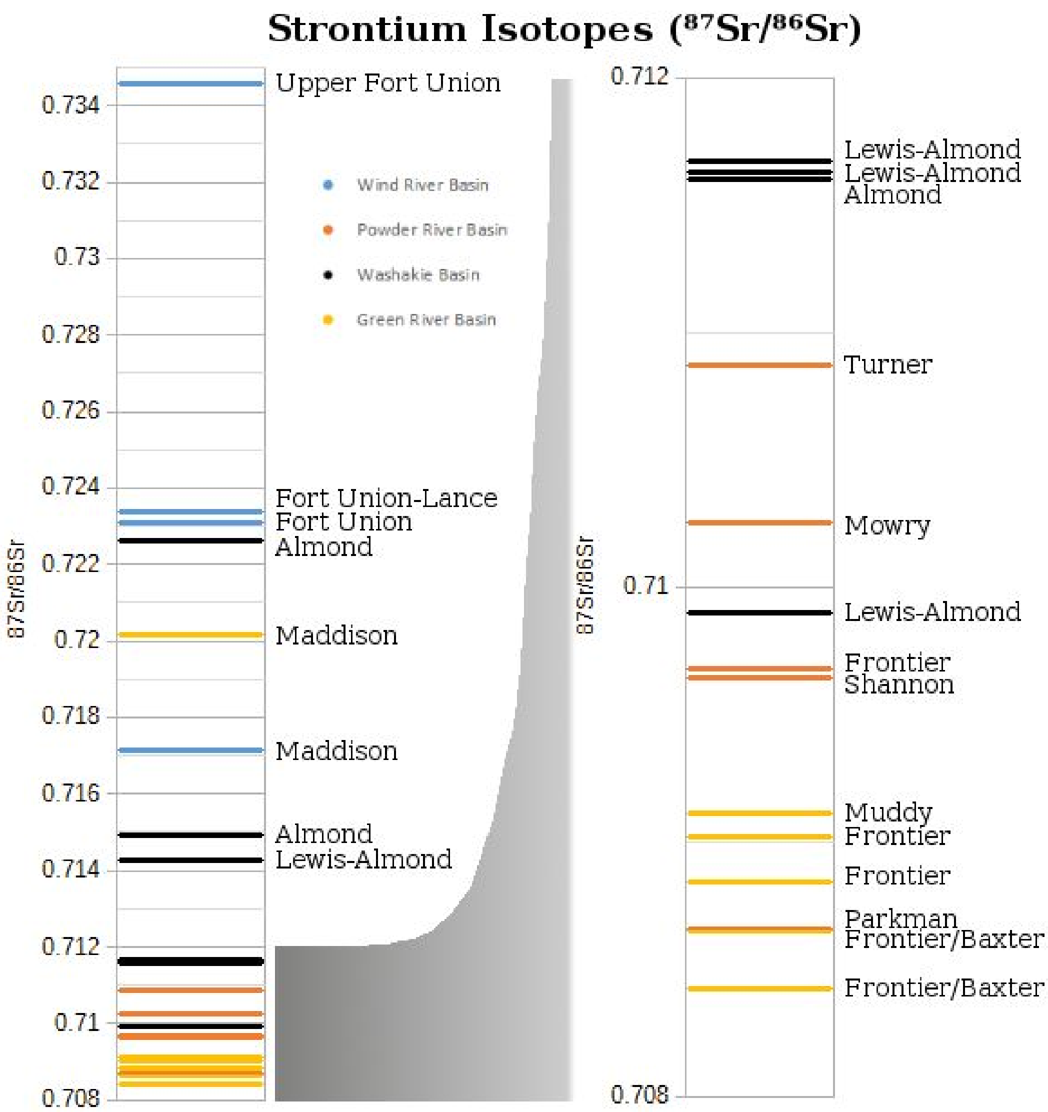

Figure 9: A univariate plot of Strontium ratios (left), and enlarged detail of that plot (right). The colors used here match the colors used for the basins elsewhere in this report. Note that formations such as the Madison or Frontier plot near each other, even if they sample different basins. This is due to the composition of the reservoir formation being consistent over large lateral distances, and transferring strontium isotopes to the water in a similar ratio.

Conclusions:

A few decades ago REEs were believed to be insoluble except in exotic solutions. While it is true that REEs contribute only a small part of the ions found in natural aqueous solutions, they nevertheless are a measurable component. This project has shown that REEs are measurable species in terrestrial geothermal waters and also terrestrial oil and gas thermal waters at the nanograms per litre level. Further, this project has shown that measurement of REEs is possible with industry standard equipment using the method of McLing et al. (2014) despite barium, hydrocarbon, and salt interferences.

While measuring REEs this project achieved a 33-fold improvement in minimal sample size over the methods of Strachan et al. (1989) and McLing et al. (2014). This improvement was made possible by the Department of Energy's involvement in this project, and grants owners of low-volume sample catalogues access to analysis of REE concentrations by a method which previously required a prohibitively large volume of sample.

The focus of this project to date has been to collect and analyse samples rather than interpret conclusions. However, the team incidentally found four conclusions:

1) In about a third of the samples Europium is the most abundant REE rather than Lanthanum. This abundance is apparent especially after normalization where all OGTWs have a significant Europium positive anomaly (NASC Eu/Eu* >> 3). In some samples this anomaly can exceed 40 times the nominal NASC Eu/Eu* anomaly.
2) Our data suggest that aqueous REEs can serve as basin-scale tracers of water in much the same way as REEs are tracers for rock. While generally more variable than in rock, aqueous REEs appear to record this basin-wide signature in their LREE:HREE ratio and in the proportions of the MREEs Sm, Eu, and Gd. This basin signature most likely reflects the marine or terrestrial depositional environment of the host rock, but could also record the presence of microbes, or fracking proppants.
3) Many water samples have higher REE concentrations than ocean water, and every water sample exceeds ocean water in at least one REE. These superior concentrations do not necessarily imply a better resource because other factors may affect resource viability. Extraction from OGTWs would need to solve problems not present in the ocean such as entrained oil droplets and disposal of the post-extraction water. On the other hand, some benefits such as the geothermal potential of OGTWs is not present in the ocean.
4) Almost all OGTWs have similar LREE behaviors, but can exhibit great variety in the HREEs. This suggests HREEs are more heterogeneously distributed in groundwater than LREEs. Because most HREEs are also critical REEs, a prospecting method that selects for HREEs would be economically valuable.

References

Alibo D.S., Y. Nozaki (1999) Rare earth elements in seawater: particle association, shale-normalization, and Ce oxidation. Geochimica et Cosmochimica Acta, 63 (3), pp. 363–372. http://dx.doi.org/10.1016/S0016-7037(98)00279-8.

Elderfield, H. and Greaves, M.J., 1982. The rare earth elements in seawater. *Nature*, 296, pp.214-219.

Guo, H., Zhang, B., Wang, G., & Shen, Z. (2010). Geochemical controls on arsenic and rare earth elements approximately along a groundwater flow path in the shallow aquifer of the Hetao Basin, Inner Mongolia. Chemical Geology, 270(1), 117-125.

Johannesson, K.H., Chevis, D.A., Burdige, D.J., Cable, J.E., Martin, J.B. and Roy, M., 2011. Submarine groundwater discharge is an important net source of light and middle REEs to coastal waters of the Indian River Lagoon, Florida, USA. *Geochimica et Cosmochimica Acta*, 75(3), pp.825-843.

Klinkhammer, G.P., Elderfield, H., Edmond, J.M. and Mitra, A., 1994. Geochemical implications of rare earth element patterns in hydrothermal fluids from mid-ocean ridges. *Geochimica et Cosmochimica Acta*, 58(23), pp.5105-5113.

Martini, A.M., Walter L.M., Budai J.M., Ku, T.C.W., Kaiser, C.J., and Schoell, M., 1998, Genetic and temporal relations between formation waters and biogenic methane: Upper Devonian Antrim Shale, Michigan Basin, USA, Geochemica et Cosmochimica Acta, v. 62, no.10 p.1699-1720.

McLing, T.L., Smith, W.W., and Smith R.W., 2014 Utilizing REEs as Tracers in High TDS Reservoir Brines in CCS Applications. Energy Proceedia, Volume 63, 2014, Pages 3963–3974

McLaughlin, J.F., Frost, C.D., Sharma, S., 2011, Isotopic analysis of Atlantic Rim waters, Carbon County, Wyoming: A new tool for characterizing coalbed natural gas systems. AAPG Bulletin

Migdisov A., A.E. Williams-Jones, J. Brugger, F.A. Caporuscio. (2016) Hydrothermal transport, deposition, and fractionation of the REE: experimental data and thermodynamic calculations. Chemical Geology, 439, pages 13–42. http://dx.doi.org/10.1016/j.chemgeo.2016.06.005.

Nelson, B. J., Wood, S. A., & Osiensky, J. L. (2004). Rare earth element geochemistry of groundwater in the Palouse Basin, northern Idaho–eastern Washington. Geochemistry: Exploration, Environment, Analysis, 4(3), 227-241.

Nozaki Y. (2001). Rare Earth Elements and their Isotopes in the Ocean. Encyclopedia of Ocean Science, Academic Press, 2001, pp. 2354-2366. http://dx.doi.org/10.1006/rwos.2001.0284.

Quillinan S.A., and Frost, C.D., (2012), Geochemical and Stable Isotopic Analysis of teh Tongue River and Associated Tributaries in the Powder River Basin: An analysis of the Cause of Annual Elevated Salinity in Spring Runoff, Wyoming State Geological Survey Report of Investigation No. 63, 2012 ISBN 978-1-884589-57-7

Quillinan S.A., and Frost, C.D., (2013) Carbon isotope characterization of Powder River Basin coalbed waters: Key to minimizing unnecessary water production and implications for exploration and production of biogenic gas, in Karacan, C.O., Soeder, D., and Engle, M., Environmental Geology and the Unconventional Gas Revolution, International Journal of Coal Geology

Sharma S., and Frost, C. 2008, An innovative Approach for Tracing Coalbed Natural Gas Co-Produced Water Using Stable Isotopes of Carbon and Hydrogen. Groundwater, vol. 46, no. 2 March-April 2008, pp. 329-334.

Wood, S. A. (2002). Behavior of Rare Earth Element In Geothermal Systems; A New Exploration/Exploitation Tool (No. DOE/ID13575). University of Idaho (US)

Appendix:

Appendix A:

General Information and Identity (1/2)						
Sample ID	Operator	API	Longitude (°)	Latitude (°)	Formation	Name
MD-2	Aethon	4901320136 and 30 more	-107.66126	43.17729	Fort Union	Iron Horse- Water Transfer Facility
MD-3	Aethon	49-013-23395	-107.67854	43.18130	Upper Fort Union	GBU 18-41BH (feeds to West West)
MD-4	Aethon	4901322441 and 69 more	-107.65155	43.16110	Fort Union	West West
MD-5	Aethon		-107.56124	43.16368		Input brine before Osmosis
MD-6	Aethon		-107.56124	43.16368		Waste brine after Osmosis
MD-7	Aethon	49-013-22808	-107.54314	43.17356	Fort Union	GBU 17-34 (feeds to Pit 7)
MD-8	Aethon	4901306169 and 130 more	-107.50378	43.18213	Fort Union-Lance	Pit 7
PRB-10	Devon	49-005-61623	-105.47801	43.76701	Niobrara	Durham Ranches 264472-1NH
PRB-11	Devon	49-005-61885	-105.50578	43.69528	Turner	State Cosner 164372-4TH
PRB-12	Devon	49-005-62029	-105.50917	43.70812	Parkman	State Cosner 164372-3PH
PRB-13	Devon	49-005-62654	-105.50820	43.69301	Turner	Cosner Fed 21-284372-4XTH
PRB-14	Devon	49-005-62145	-105.51822	43.69309	Parkman	Cosner Fed 21-284372-2XPH
PRB-15	Devon	49-005-61648	-105.93039	43.56043	Mowry	State Iberlin Ranch 3626-4MH
PRB-16	Devon	49-005-61661	-105.94487	43.56106	Niobrara	State Iberlin Ranch 3626-1NH
PRB-17	Devon	49-005-61086	-105.94261	43.56103	Shannon	Cottonwood 3626-2SH
PRB-18	Devon	49-005-61746	-105.99433	43.57488	Frontier	Iberlin Ranch Federal 2826-4FH
PRB-19	Devon	49-005-61725	-105.99444	43.57478	Frontier	Iberlin Ranch Federal 3326-3FH
DJPP-20	PacifiCorp		-105.77511	42.84581	Surface pond	Dave Johnson Upper Ash pond
DJPP-21	PacifiCorp		-105.77511	42.84581	Surface pond	Dave Johnson Upper Ash pond
WYDAK-22	PacifiCorp		-105.39047	44.28856	Surface pond	Wyodak Upper Ash pond
WYDAK-23	PacifiCorp		-105.39095	44.29081	Surface pond	Wyodak coal pond
WYDAK-24	PacifiCorp		-105.39523	44.28936	Surface pond	Wyodak Lower Ash pond
WYDAK-25	PacifiCorp		-105.38557	44.28713		Wyodak fly-ash-removal truck
LR-27	Mo. Bsn Pwr Prjct		-104.89611	42.11005	Surface pond	Lowest Pond
LR-28	Mo. Bsn Pwr Prjct		-104.89577	42.10993	Surface pond	Low Pond
LR-29	Mo. Bsn Pwr Prjct		-104.89746	42.10843	Surface pond	High pond
LR-30	Mo. Bsn Pwr Prjct		-104.88245	42.11686	Surface pond	Emergency west pond
LC-31	Conoco Phillips	4901321917 and 7 more	-107.60692	43.27848	Madison	Lost Cabin flash drum Sample
JBPP-32	PacifiCorp		-108.78	41.74	Surface pond	Jim Bridger fly ash wet scrubber

General Information and Identity (2/2)						
Sample ID	Operator	API	Longitude (°)	Latitude (°)	Formation	Name
WA-33	Well Location, Ownership, and Other Identifying Information Restricted by NDA				Lewis-Almond	North Wamsutter Area
WA-34					Almond	North Wamsutter Area
WA-35					Lewis-Almond	North Wamsutter Area
WA-36					Almond	North Wamsutter Area
WA-37					Almond	North Wamsutter Area
WA-38					Lewis-Almond	South Wamsutter Area
WA-39					Almond	South Wamsutter Area
WA-40					Lewis-Almond	South Wamsutter Area
LB-42	Exxon Mobile	16 wells	-110.352	42.373	Maddison	Maddison pre-filter
LB-43	Exxon Mobile	49-035-22225	-110.31514	42.33017	Frontier/Baxter	Hogsback 33-18 G1
LB-44	Exxon Mobile	49-035-06320	-110.31943	42.28774	Muddy	Hogsback 32-31
LB-45	Exxon Mobile	49-023-05230	-110.30713	42.26140	Frontier/Baxter	Hogsback 77-6
LB-46	Exxon Mobile	49-035-21297	-110.24731	42.38269	Frontier	Tip-top 86-27 G1
LB-47	Exxon Mobile	49-035-21267, 49-035-21265	-110.29559	42.40184	Frontier	Tip-top 43-20 G1 & G2
LB-48	Exxon Mobile	49-035-20058	-110.34503	42.42192	Muddy	Tip Top 18-12
MS-50	Burlington Rsrcs	49-013-21663	-107.61418	43.28837	Mesa-Verde	Mary Federal 5-3
MS-51	Burlington Rsrcs	49-013-20277	-107.62443	43.28631	Lower Fort Union	MDU-8
MS-52	Burlington Rsrcs	49-013-23131	-107.62378	43.28333	Lower Fort Union	MDU-161-D
MS-53	Burlington Rsrcs	49-013-20745	-107.63624	43.29075	Lance	Spcatt 1-4
MS-54	Burlington Rsrcs	49-013-20425	-107.62485	43.29084	Lance	MDU-1-3
MS-55	Burlington Rsrcs	Multiple	-107.62368	43.29283	Gather-Station	SWDD Oakie-FEE
MS-56	Burlington Rsrcs	49-013-21837	-107.62109	43.30130	Lance	Thomas 2-34
MS-57	Burlington Rsrcs	49-013-22989	-107.65547	43.29128	Lower Fort Union	MDU-208-D
MS-58	Burlington Rsrcs	49-013-20897	-107.74323	43.30643	Cody	Quincy-1-34 (MDU 1-34)
MS-59	Burlington Rsrcs	49-013-21161	-107.73797	43.30392	Cody	Quincy-2-34

Appendix B:

Collection Information (1/2)					
Sample ID	pH (units)	Cond (mS)	Temp (°C)	ORP (mV)	On-site Field Notes
MD-2	9.57	7.721	11		Gather station of many wells
MD-3	7.23	8.385	36		A single well. GBU abbreviates Gun Barrel Unit
MD-4	7.3	5.706	25.2		Gather station of many wells
MD-5	6.98	2.969	29.6		Garage sample point, next to sand-filter. Water from West West (MD-4)
MD-6	10.01	217	35.3		Main Floor sample point, next to pipe rack. Water from West West (MD-4)
MD-7	7.63	4.446	65.4		A single well. GBU abbreviates Gun Barrel Unit
MD-8	7.26	2.039	52.1		Gather station of many wells
PRB-10	7.3	4.619	16.7		Very little sample produced.
PRB-11	6.87	15.2	34.6		Brown-yellow, oil is dispersed pretty evenly, some floating particles, and some petrol smell
PRB-12	7.94	11.23	52.3		Many large bubbles on the surface, strong petrol small, warm temp, caramel color
PRB-13	6.79	9.923	53.4		Small-dark particles floating/sinking/suspended, many large bubbles, greenish-light brown
PRB-14	7.69	5.078	50.4		Same gathering station/site as PRB-13 but different well
PRB-15	7.01	5.3	40		Mostly clear with some yellowish-tint, small soap bubbles, no visible particulate
PRB-16	6.53	5.735	40		Clear some large particles, yellowish, some soap bubbles
PRB-17	6.91	4.276	34		Greenish-brown odd smell, not H2S?, sour-gas? Few bubbles, some large particles.
PRB-18	6.63	2.976	34		Clear no strong smell, well mixed, this is a horizontal well
PRB-19	6.72	4.172	44		clear, strong smell. Same location as PRB-18, but goes horizontal in opposite direction
DJPP-20	8.5	0.147	20		Two bottles, same source: this one from before bottom ash dumping
DJPP-21					Two bottles, same source: this one during bottom-ash dumping
WYDAK-22	8.71	0.8138	14.5		Water recirculates with little/no processing, no bottom ash was dumping during collection.
WYDAK-23	7.54	0.8179	10.3		Water unrelated to ash. Drains the upper wyodak coal seam (lots of plants on water's edge)
WYDAK-24	9.07	0.3285	12.4		Upper ash pond empties into lower ash pond, which is in contact with old ash
WYDAK-25	10.85	1.018	14.3		Contains a mix of fly ash and lime. Fly ash washed off scrubber less than a minute ago.
LR-27	8.35	2.33	3.5		Evaporation only. Never pumped out. Low Pond may have been slowly draining into Lowest.
LR-28	8.39	0.9299	5.3		Water recycled to plant, or occasionally released to lowest pond. near pipe to lowest pond
LR-29	9.4	0.3404	4.8		Water from plant used to carry ash out for settling, collected near pipe to low pond
LR-30	7.89	2.015	3.5		Contains water from treatment center. Separate from the other ponds.
LC-31	6.5		20		4901321917 and 4901322127 make vast majority, other six are minor condensate
JBPP-32					Collected by plant employee at the end of a visit by CMI. unknown collection procedure.

Collection Information (2/2)					
Sample ID	pH (units)	Cond (mS)	Temp (°C)	ORP (mV)	On-site Field Notes
WA-33	7.5	11.11	15.9	-66	Cloudy, strong petrol odor, cool to touch, contains solid separates
WA-34	7.8	9.2	15.7	-148	8 wells to two separators. White and cloudy, less petrol odor, no visible solids.
WA-35	7.07	16.47	18.8	-69	Large black solid separates, otherwise clean. Condensate layer floats on surface.
WA-36	6.86	20.65	23.4	-36	Recollected to be more representative
WA-37	6.84	15.55	17.9	-20	Floating layer white-grey and cloudy, oil on surface, strong petrol scent.
WA-38	7.48	30.65	24		South of interstate now. Mostly condensate. Dark orange, difficult to get any water out.
WA-39	7.1		28.2		Methonol and soap added as surfactants. Much foam. Visible outgassing (heat-wave texture)
WA-40	6.64	10.1	26.2		Sample collected from tanks, grey cloudy, strong petrol odor, floating black particles.
LB-42	6.08	2.257	18.6	-244	Taken by employee using our bottles before the main filter, but after pre-filter.
LB-43	4.94	3.5	5.5	143	Meter would not settle on a conductivity value, suspect interference.
LB-44	4.98	0.1	8	101	Like all LB samples, taken from water-tank pit
LB-45	8.39	9.843	9.1	58	Guide suggests normal TDS is ~8300 ppm
LB-46	5.75	31.5	9.9	95	Took large sample for analytical method development
LB-47	5.8	16.8	10.8	94	Much condensate. Tank was being filled during sampling
LB-48	3.79	0.96	5	295	Almost all Oil or Condensate no water.
MS-50	7.85	21.4	54	134	203F on inline. Well uses a chiller before seporator
MS-51	6.97	11.98	55	108	unknown temp on inline (no gap in insulation to measure by infrared)
MS-52	6.75	18	31	-2	112.5F on inline
MS-53	6.24	0	14.5	100	55F on inline. Looks like condensate, noticeably low density, slippery.
MS-54	7.65	13.7	63.1	-97	190F on inline. A lot of black specks. Otherwise unusually clean.
MS-55	7.29	28.6	37.8	-64	unknown temp on inline (no gap in insulation to measure by infrared)
MS-56		12.3	6.71	-50	unknown temp on inline (no gap in insulation to measure by infrared)
MS-57	6.78	12.14	33.7	-31	unknown temp on inline (no gap in insulation to measure by infrared)
MS-58	6.84				Taken from Tank bottom (truck outlet)
MS-59	6.84	31	24.5	7	Taken from Tank bottom (truck outlet) 55F inline

Appendix C:

Anions (1/2)								
Sample ID	Alkalinity, Total as CaCO3 (ppm)	Bromide (ppm)	Chloride (ppm)	Fluoride (ppm)	Ammonia as N (ppm)	Nitrate+Nitrite as N (ppm)	Phosphate as P (ppm)	Sulfate (ppm)
MD-2	4500	3	633	1.3	8.6	0.1	ND	ND
MD-3	3410	15	1190	1	42	ND	0.4	5
MD-4	3390	11	1550	1.8	9.9	ND	ND	4
MD-5	2550	17	2040	1.8	5.5	ND	0.3	ND
MD-6	4950	134	19600	10	6.4	ND	4.9	19700
MD-7	1930	13	2030	2.1	3.7	ND	ND	15
MD-8	2020	15	2060	2	5.2	ND	0.4	ND
PRB-10	268						0.8	
PRB-11	267	355	35600	0.5	44	ND	ND	ND
PRB-12							19.2	
PRB-13	323	349	37800	0.5	49	ND	ND	ND
PRB-14	1440	89	11100	1.9	11.5	ND	1.6	ND
PRB-15	425	293	33000	1	33	ND	1.8	ND
PRB-16	256	558	44600	1	63	ND	14.6	ND
PRB-17	519	714	45900	0.8	28	ND	5.6	ND
PRB-18	219	261	24300	0.7	31	ND	1.8	ND
PRB-19	223	398	31200	0.5	38	ND	ND	ND
DJPP-20	160	ND	16	0.3	ND	ND	ND	183
DJPP-21	159	ND	17	0.3	ND	ND	ND	184
WYDAK-22	275	4	765	2.3	0.5	4.1	ND	1200
WYDAK-23	148	5	547	0.2	ND	0.6	ND	2430
WYDAK-24	54	9	522	0.8	0.13	1.2	ND	1840
WYDAK-25	72	158	1050	1	ND	6.2	ND	1880
LR-27	578	116	18600	94	18	1.3		88200
LR-28	48	ND	199	0.6	0.22	0.3		1400
LR-29	37	2	225	0.4	0.15	0.4		1590
LR-30	194	93	2250	37	13	5.3		14500
LC-31	1830	ND	8350	6.6	45	ND		ND
JBPP-32	55000	332	5870	417	ND	4		165000

Anions (2/2)								
Sample ID	Alkalinity, Total as CaCO3 (ppm)	Bromide (ppm)	Chloride (ppm)	Fluoride (ppm)	Ammonia as N (ppm)	Nitrate+Nitrite as N (ppm)	Phosphate as P (ppm)	Sulfate (ppm)
WA-33	2070	28	2630	6			0.4	260
WA-34	2460	17	1760	8			ND	243
WA-35	1900	49	4970	13			0.2	253
WA-36	954	48	6440	12			ND	184
WA-37	2190	42	4530	13			0.2	348
WA-38	1410	98	4280	8			0.6	995
WA-39	2050	ND	763	13			0.4	438
WA-40	1190	15	1930	16			ND	283
LB-42	187	1	474	0.3			ND	32
LB-43	276	ND	1620	ND			ND	ND
LB-44	472	5	2270	ND			ND	10
LB-45	1881	12	1830	2			ND	ND
LB-46	103	17	12400	ND			ND	ND
LB-47	181	8	4920	ND			ND	ND
LB-48								
MS-50	1095.6	64.9	6787	2.2				ND
MS-51	2244	26.4	3157	1.98				ND
MS-52	1639	24.2	2827	1.98				16.5
MS-53								
MS-54	2189	19.8	2277	2.31				16.5
MS-55	1738	37.4	4202	2.2				ND
MS-56	784.3	14.3	1628	1.43				7.7
MS-57	1683	20.9	2519	1.1				13.2
MS-58	352	116.6	11990	5.5				ND
MS-59	610.5	40.7	3410	2.2				ND

Appendix D:

	Cations (1/2)				Trace Elements (1/2)									
Sample ID	Calcium (ppm)	Magnesium (ppm)	Potassium (ppm)	Sodium (ppm)	Aluminum (ppm)	Barium (ppm)	Boron (ppm)	Iron (ppm)	Lithium (ppm)	Manganese (ppm)	Molybdenum (ppm)	Phosphorus (ppm)	Silicon (ppm)	Strontium (ppm)
MD-2	1	ND	40	2590	ND	0.54	7.34	0.25	2.5	ND	0.002	ND	3.5	0.05
MD-3	16	13	57	3510	ND	23.5	3.82	0.16	3.8	0.025	ND	0.4	27.7	0.79
MD-4	18	3	27	2480	ND	7.36	9.1	0.08	2.2	0.014	ND	0.1	35.5	0.97
MD-5	22	3	23	2500	0.18	5.92	11.2	0.08	1.8	0.011	ND	0.3	39.1	1.15
MD-6	3	ND	183	23200	0.04	0.12	82.7	0.07	13.8	ND	ND	4.9	164	0.05
MD-7	17	2	17	2200	ND	3.49	10.1	0.09	1.2	ND	ND	ND	38.4	0.91
MD-8	20	2	18	2160	ND	4.33	11.8	0.08	1.4	0.016	ND	0.4	35.7	1.07
PRB-10	734	72	95	13000	ND	83.9	22.9	1.99	5.9	2.26	ND	0.8	6	64
PRB-11	2290	180	208	22300	ND	246	15.7	12.7	14.6	0.53	ND	ND	42.1	171
PRB-12	83	9	115	5100	ND	8.85	9.8	4.5	0.8	0.21	ND	19.2	17.1	7.9
PRB-13	2340	171	1170	20100	ND	204	19	57.3	14.4	1.15	ND	ND	47.5	164
PRB-14	60	13	258	5970	ND	14.4	11.2	0.4	0.9	0.08	ND	1.6	22.7	12.3
PRB-15	1680	98	76	15900	ND	42.1	30.5	1.6	8.9	0.85	ND	1.8	73.3	111
PRB-16	814	74	79	13700	ND	65.1	29.8	25	6.7	0.51	ND	14.6	68.6	84.9
PRB-17	386	56	119	17000	ND	177	17.7	5.6	5.1	0.19	ND	5.6	37.7	87.8
PRB-18	1770	72	181	13200	ND	113	13.6	0.9	10.2	0.476	ND	1.8	55	135
PRB-19	2560	127	245	15500	0.4	145	11	26.6	11.1	1.4	ND	ND	34.7	187
DJPP-20	64	25	4	68	0.2	0.1	0.09	ND	ND	ND	ND	ND	0.9	0.61
DJPP-21	68	26	4	60	0.29	0.07	0.1	ND	ND	0.018	0.003	ND	1.3	0.67
WYDAK-22	180	33	29	945	1.27	0.19	1.61	0.19	ND	0.052	0.099	ND	2.1	3.61
WYDAK-23	459	151	45	840	0.07	0.07	1.16	0.06	ND	0.049	0.005	ND	4	5.38
WYDAK-24	344	40	50	824	0.75	0.12	1.36	0.03	ND	0.007	0.149	ND	2.3	5.32
WYDAK-25	145	1	48	1310	6.82	0.11	1.13	ND	ND	ND	0.278	ND	2.4	3.81
LR-27	507	5430	2190	19200	ND	0.17	28.4	ND	4.5	3.05	2	ND	ND	25.4
LR-28	198	9	60	549	1.91	0.08	1.15	ND	ND	0.002	0.16	0.5	ND	6.4
LR-29	232	6	70	624	5.39	0.07	1.32	ND	ND	0.004	0.17	0.7	ND	7.81
LR-30	385	1510	485	4950	ND	0.08	6	0.1	1.5	4.79	0.331	ND	7	2.85
LC-31	2	ND	56	379	0.5	0.23	10.1	ND	1.4	0.027	0.01	ND	4	0.31
JBPP-32	60	130	996	81400	28	0.51	276	5.8	4.4	0.224	9.3	160	120	1.89

	Cations (2/2)				Trace Elements (2/2)									
Sample ID	Calcium (ppm)	Magnesium (ppm)	Potassium (ppm)	Sodium (ppm)	Aluminum (ppm)	Barium (ppm)	Boron (ppm)	Iron (ppm)	Lithium (ppm)	Manganese (ppm)	Molybdenum (ppm)	Phosphorus (ppm)	Silicon (ppm)	Strontium (ppm)
WA-33	23	4	32	2520	0.04	2.19	12.4	ND	0.8	0.074	ND	0.4	21	3.98
WA-34	8	2	25	2170	0.04	2.15	5.92	ND	0.8	0.025	0.004	ND	22	2.38
WA-35	30	7	32	3440	0.03	15.3	14.6	ND	2.4	0.034	0.002	0.2	37	4.6
WA-36	70	ND	35	414	ND	3.31	16.2	ND	2.5	0.036	ND	ND	36	0.26
WA-37	34	7	29	3510	0.04	7.48	16.8	0.3	1.7	0.05	0.002	0.2	39	0.68
WA-38	23	6	59	3220	ND	0.23	14.4	ND	0.9	0.1	0.044	0.6	18	3.33
WA-39	5	2	16	1270	0.04	1.46	12.4	0.4	0.9	0.04	0.01	0.4	40	0.32
WA-40	5	1	37	1780	ND	0.96	13.9	1.3	1.6	0.22	0.342	ND	43	1.62
LB-42	8	2	47	320	ND	ND	6.4	0.15	1.6	0.17	ND	ND	1.3	0.5
LB-43	46	7	69	1150	0.09	5.68	1.1	166	0.2	26.7	ND	ND	0.4	5.47
LB-44	49	12	45	1690	ND	4.08	1.6	626	0.3	31.7	ND	ND	2.8	6.77
LB-45	2	ND	25	1950	ND	2.6	3.9	2.2	0.3	0.022	0.003	ND	7	0.86
LB-46	800	65	121	6040	0.2	106	2.6	31.1	2.3	2.23	ND	ND	3.7	89
LB-47	211	25	79	2990	ND	11.1	3.4	1.6	1.3	0.97	0.002	ND	5	24.5
LB-48														
MS-50	34	2	74	3890	ND	9.45	93.4	ND	10.6	0.014	0.003	ND	60.9	23.1
MS-51	21	4	32	2860	ND	10.3	11.8	0.15	1.3	0.035	0.002	ND	24.6	1.89
MS-52	13	4	19	2830	ND	4.5	25.5	0.11	1.9	0.007	ND	ND	45.3	1.03
MS-53														
MS-54	13	1	15	2120	ND	5.12	20	0.11	2.3	0.005	0.001	2.6	48.3	4.22
MS-55	22	2	43	2960	ND	7.16	48.1	0.05	5.4	0.01	ND	1.9	22	11
MS-56	9	1	9	1410	ND	1.75	12.2	ND	0.9	0.004	ND	ND	14	1.59
MS-57	11	3	13	1680	ND	2.61	11	ND	0.9	0.006	ND	ND	21.5	0.71
MS-58	104	6	201	6090	ND	36.7	79.7	3	13.2	0.332	0.003	ND	19.6	64.6
MS-59	29	3	23	2340	ND	6.01	30.5	0.11	2.4	0.156	0.042	0.2	25.9	3.93

Appendix E:

REE post normalization to NPDW (1/2)

Sample ID	La (ratio)	Ce (ratio)	Pr (ratio)	Nd (ratio)	Sm (ratio)	Eu (ratio)	Gd (ratio)	Tb (ratio)	Dy (ratio)	Ho (ratio)	Er (ratio)	Tm (ratio)	Yb (ratio)	Lu (ratio)
MD-2	14.2089	129.2655	20.3086	13.4352	6.1225	22.9109	5.6044	2.9708	1.7181	1.1650	0.9928	0.7726	0.4989	0.6568
MD-3	4.4942	38.7855	6.1878	4.0649	2.9946	59.7141	2.5974	1.3394	0.8938	0.6535	0.4765	0.3510	0.2844	0.2533
MD-4	4.0046	34.5154	5.4612	4.6004	11.9021	351.1112	9.5766	1.5111	0.8695	0.8226	0.7286	0.9677	0.7852	1.0355
MD-5	2.5679	11.5053	1.4969	1.4697	11.6645	393.8270	9.4231	0.6321	0.4033	0.3958	0.3573	0.6347	0.4172	0.8048
MD-6	1.0167	3.4548	0.3898	0.2016	0.4542	3.4743	0.1426	0.2700	0.1841	0.1817	0.1661	0.2297	0.1471	0.1628
MD-7	2.6308	20.2850	3.0544	3.0904	11.1589	361.4787	8.9744	1.3536	0.6663	0.6203	0.4618	0.7916	0.4915	0.7605
MD-8	1.3299	5.3951	0.8032	0.8690	8.2102	300.8834	6.6998	0.3149	0.4747	0.3010	0.3865	0.4080	0.3880	0.5732
PRB-10	3.5976	6.1274	0.6527	0.4821	1.6764	84.6036	18.0115	0.2669	0.1853	0.1899	0.1954	0.4773	0.2516	1.2289
PRB-11	3.7386	12.3372	1.5971	1.0528	1.4901	45.1524	10.7561	0.3067	0.1777	0.1880	0.1722	0.3098	0.1842	0.7244
PRB-12	0.6191	3.0097	0.4134	0.2502	0.2027	4.8987	1.0979	0.1379	0.0929	0.1024	0.0699	0.1301	0.0561	0.1345
PRB-13	0.2590	4.1919	0.1729	0.0949	0.1333	2.7408	0.7138	0.0727	0.0380	0.0536	0.0573	0.0858	0.0577	0.0827
PRB-14	0.1535	1.0089	0.1322	0.0644	0.5125	3.7916	1.0690	0.3968	0.7053	0.7301	0.7540	0.8053	0.6627	0.7677
PRB-15	0.4145	1.4478	0.1626	0.0912	0.2728	7.4009	1.9183	0.4771	2.1308	5.3987	10.5744	12.7751	12.2926	13.9011
PRB-16	3.1116	8.0476	1.0397	0.5979	1.1655	16.4349	5.0281	0.9816	1.6051	2.2425	3.1744	4.5821	4.8590	7.1793
PRB-17	4.2015	3.3840	0.8348	0.2298	0.9432	52.7317	12.3419	0.3031	0.5025	0.9433	1.8984	2.9364	3.3408	5.1316
PRB-18	1.3624	1.5986	0.2365	0.1976	0.4534	22.5683	6.0675	0.1643	0.1805	0.1918	0.1718	0.3926	0.2654	0.5914
PRB-19	0.0890	0.3885	0.0617	0.0166	ND	0.1673	0.0530	0.0352	0.0364	0.3009	2.3820	6.8489	10.3485	15.5868
DJPP-20														
DJPP-21														
WYDAK-22	2.2145	67.3153	10.3209	13.7880	21.8978	32.1568	26.2969	28.8985	31.2967	30.6425	31.1636	28.6729	29.7835	29.7452
WYDAK-23	3.8385	36.7477	5.7485	6.3130	11.7700	14.2736	11.5551	15.3638	16.9910	20.6037	30.6128	42.6170	61.7389	87.8383
WYDAK-24	1.0962	13.9186	2.1348	2.7244	4.0165	9.0684	4.8639	4.7622	4.2334	3.5784	3.5570	3.1607	3.6974	4.7368
WYDAK-25	0.4756	16.5607	2.6431	3.0318	4.0325	14.5721	4.5564	3.7921	3.4846	3.3612	4.2664	4.5813	4.9260	6.3523
LR-27	1.8256	7.9261	1.3962	0.9187	0.7314	1.3880	ND	1.1448	1.0019	1.2926	1.6180	2.0499	2.2190	3.2694
LR-28	2.4413	31.1808	4.4041	4.0063	3.2092	6.4241	1.9366	2.2615	1.7400	1.3750	1.4481	1.8279	2.1445	2.9479
LR-29	7.4710	89.4504	13.4368	11.1045	8.8676	9.5344	6.6130	6.1835	4.6179	3.2265	2.8858	2.8698	2.9379	3.1217
LR-30	6.1539	33.8478	5.3675	2.3693	0.8516	2.1457	1.4280	1.7652	2.5912	3.8347	6.0906	7.6236	9.5581	12.9112
LC-31	8.7524	44.7146	6.8714	3.9494	2.6295	5.0319	3.1687	4.2179	7.6449	11.6415	21.3965	36.4370	43.4088	37.2985
JBPP-32	0.0754	52.9020	0.8581	13.2137	0.2987	0.8394	0.3236	0.4231	0.0476	0.0448	0.0517	0.0377	0.0244	0.0537

REE post normalization to NPDW (2/2)

Sample ID	La (ratio)	Ce (ratio)	Pr (ratio)	Nd (ratio)	Sm (ratio)	Eu (ratio)	Gd (ratio)	Tb (ratio)	Dy (ratio)	Ho (ratio)	Er (ratio)	Tm (ratio)	Yb (ratio)	Lu (ratio)
WA-33	0.4883	6.0457	1.3918	1.1742	4.2974	217.8684	3.5689	0.5928	0.6572	0.6274	0.3905	0.9144	0.6489	1.3755
WA-34	0.5973	0.8730	0.1853	0.3382	4.0656	195.2691	3.2772	0.5266	0.1556	0.2450	0.1031	0.4551	0.1433	0.3702
WA-35	0.3717	5.5270	1.3485	1.4607	18.1758	637.3739	14.2541	0.6144	0.6995	0.6659	0.5766	0.9213	0.7834	1.2403
WA-36	2.3556	7.9880	0.7678	1.2621	12.6209	599.8903	10.2456	0.7593	1.0194	1.1485	1.3092	1.5430	1.6137	1.7585
WA-37	0.8895	3.1893	0.2808	0.5489	5.8024	282.9373	4.7503	0.5174	0.3274	0.3590	0.4095	0.5340	0.6627	0.9582
WA-38														
WA-39														
WA-40	0.8001	10.2354	2.2439	1.4362	2.0000	82.7754	1.7373	0.5267	0.7912	0.4259	0.6946	1.4091	3.3450	8.7436
LB-42	1.0715	13.8773	1.8025	0.9980	1.1775	1.8954	1.5578	1.1046	0.8344	0.7778	0.6378	0.7166	0.5926	0.7864
LB-43	7.3086	89.2322	5.7477	3.2021	4.1924	3.5583	1.7462	1.7735	1.6985	1.5193	1.4837	1.2132	1.0149	1.0028
LB-44	5.3179	67.0963	4.8802	3.0551	3.5376	100.3050	3.3082	1.7382	1.4635	1.0953	0.8556	0.6598	0.5907	0.6375
LB-45	0.9477	12.3240	1.6897	1.4066	3.4969	121.2011	2.8132	0.9232	0.8936	0.5831	0.5534	0.5808	0.6276	0.7503
LB-46														
LB-47	1.0083	4.1578	0.1295	0.5011	8.2660	413.4765	6.7816	0.5183	0.0684	0.2412	0.0701	0.4480	0.2122	0.4847
LB-48														

Appendix F:

REEs before normalization (1/2)														
Sample ID	La (ng/L)	Ce (ng/L)	Pr (ng/L)	Nd (ng/L)	Sm (ng/L)	Eu (ng/L)	Gd (ng/L)	Tb (ng/L)	Dy (ng/L)	Ho (ng/L)	Er (ng/L)	Tm (ng/L)	Yb (ng/L)	Lu (ng/L)
MD-2	76.384	72.088	14.595	46.122	4.152	4.317	6.019	0.534	2.340	0.450	1.318	0.161	0.755	0.168
MD-3	24.160	21.630	4.447	13.954	2.031	11.252	2.790	0.241	1.217	0.252	0.633	0.073	0.430	0.065
MD-4	21.528	19.248	3.925	15.793	8.071	66.160	10.285	0.271	1.184	0.317	0.968	0.201	1.188	0.265
MD-5	13.805	6.416	1.076	5.045	7.910	74.209	10.121	0.114	0.549	0.153	0.474	0.132	0.631	0.206
MD-6	5.466	1.927	0.280	0.692	0.308	0.655	0.153	0.048	0.251	0.070	0.221	0.048	0.222	0.042
MD-7	14.143	11.313	2.195	10.609	7.567	68.114	9.639	0.243	0.907	0.239	0.613	0.164	0.743	0.194
MD-8	7.149	3.009	0.577	2.983	5.568	56.696	7.196	0.057	0.646	0.116	0.513	0.085	0.587	0.146
PRB-10	19.340	3.417	0.469	1.655	1.137	15.942	19.345	0.048	0.252	0.073	0.259	0.099	0.381	0.314
PRB-11	20.098	6.880	1.148	3.614	1.010	8.508	11.552	0.055	0.242	0.073	0.229	0.064	0.279	0.185
PRB-12	3.328	1.678	0.297	0.859	0.137	0.923	1.179	0.025	0.127	0.040	0.093	0.027	0.085	0.034
PRB-13	1.392	2.338	0.124	0.326	0.090	0.516	0.767	0.013	0.052	0.021	0.076	0.018	0.087	0.021
PRB-14	0.825	0.563	0.095	0.221	0.348	0.714	1.148	0.071	0.960	0.282	1.001	0.167	1.002	0.196
PRB-15	2.228	0.807	0.117	0.313	0.185	1.395	2.060	0.086	2.902	2.084	14.043	2.654	18.592	3.551
PRB-16	16.727	4.488	0.747	2.052	0.790	3.097	5.400	0.176	2.186	0.865	4.216	0.952	7.349	1.834
PRB-17	22.586	1.887	0.600	0.789	0.640	9.936	13.255	0.054	0.684	0.364	2.521	0.610	5.053	1.311
PRB-18	7.324	0.891	0.170	0.678	0.307	4.253	6.517	0.030	0.246	0.074	0.228	0.082	0.401	0.151
PRB-19	0.478	0.217	0.044	0.057		0.032	0.057	0.006	0.050	0.116	3.163	1.423	15.652	3.982
DJPP-20														
DJPP-21														
WYDAK-22	11.905	37.540	7.417	47.333	14.849	6.059	28.243	5.190	42.618	11.826	41.387	5.958	45.046	7.599
WYDAK-23	20.635	20.493	4.131	21.672	7.982	2.690	12.410	2.759	23.138	7.952	40.655	8.855	93.377	22.439
WYDAK-24	5.893	7.762	1.534	9.352	2.724	1.709	5.224	0.855	5.765	1.381	4.724	0.657	5.592	1.210
WYDAK-25	2.557	9.236	1.899	10.408	2.735	2.746	4.894	0.681	4.745	1.297	5.666	0.952	7.450	1.623
LR-27	9.814	4.420	1.003	3.154	0.496	0.262		0.206	1.364	0.499	2.149	0.426	3.356	0.835
LR-28	13.124	17.389	3.165	13.753	2.176	1.210	2.080	0.406	2.369	0.531	1.923	0.380	3.243	0.753
LR-29	40.163	49.884	9.656	38.121	6.013	1.797	7.103	1.110	6.288	1.245	3.832	0.596	4.443	0.797
LR-30	33.082	18.876	3.857	8.134	0.577	0.404	1.534	0.317	3.529	1.480	8.089	1.584	14.456	3.298
LC-31	47.051	24.936	4.938	13.558	1.783	0.948	3.403	0.758	10.410	4.493	28.415	7.571	65.654	9.528
JBPP-32	0.405	29.502	0.617	45.362	0.203	0.158	0.348	0.076	0.065	0.017	0.069	0.008	0.037	0.014

REEs before normalization (2/2)														
Sample ID	La (ng/L)	Ce (ng/L)	Pr (ng/L)	Nd (ng/L)	Sm (ng/L)	Eu (ng/L)	Gd (ng/L)	Tb (ng/L)	Dy (ng/L)	Ho (ng/L)	Er (ng/L)	Tm (ng/L)	Yb (ng/L)	Lu (ng/L)
WA-33	2.625	3.372	1.000	4.031	2.914	41.053	3.833	0.106	0.895	0.242	0.519	0.190	0.981	0.351
WA-34	3.211	0.487	0.133	1.161	2.757	36.795	3.520	0.095	0.212	0.095	0.137	0.095	0.217	0.095
WA-35	1.998	3.082	0.969	5.014	12.325	120.101	15.309	0.110	0.953	0.257	0.766	0.191	1.185	0.317
WA-36	12.663	4.455	0.552	4.333	8.559	113.038	11.004	0.136	1.388	0.443	1.739	0.321	2.441	0.449
WA-37	4.782	1.779	0.202	1.884	3.935	53.314	5.102	0.093	0.446	0.139	0.544	0.111	1.002	0.245
WA-38														
WA-39														
WA-40	4.301	5.708	1.613	4.930	1.356	15.597	1.866	0.095	1.077	0.164	0.922	0.293	5.059	2.234
LB-42	5.760	7.739	1.295	3.426	0.799	0.357	1.673	0.198	1.136	0.300	0.847	0.149	0.896	0.201
LB-43	39.290	49.763	4.131	10.993	2.843	0.670	1.875	0.319	2.313	0.586	1.970	0.252	1.535	0.256
LB-44	28.588	37.418	3.507	10.488	2.399	18.901	3.553	0.312	1.993	0.423	1.136	0.137	0.893	0.163
LB-45	5.095	6.873	1.214	4.829	2.371	22.838	3.021	0.166	1.217	0.225	0.735	0.121	0.949	0.192
LB-46														
LB-47	5.420	2.319	0.093	1.720	5.605	77.912	7.284	0.093	0.093	0.093	0.093	0.093	0.321	0.124
LB-48														

Appendix G:

Stable Isotope Ratios (1/2)				
Sample ID	δ13C (ratio)	δD (ratio)	δ18O (ratio)	Sr (87/86) (ratio)
MD-2	8.30	-70.8	-3.37	
MD-3	3.31	-70.3	-1.84	0.73457
MD-4	4.13	-87.3	-3.97	
MD-5	1.13	-72.2	-2.39	
MD-6	-17.84	-43.7	1.41	
MD-7	-1.84	-68.4	-1.77	0.72311
MD-8	-0.89	-71.3	-1.90	0.72338
PRB-10	9.40	-61.3	-3.11	
PRB-11	0.82	-78.2	-7.10	
PRB-12	-8.02	-55.5	-0.87	0.70866
PRB-13	1.49	-51.6	0.81	0.71087
PRB-14	-7.34	-71.1	-6.40	
PRB-15	9.82	-70.0	-1.63	0.71025
PRB-16	4.72	-51.0	-0.34	
PRB-17	-6.87	-50.3	-2.05	0.70964
PRB-18	0.39	-51.2	-0.61	0.70968
PRB-19	2.03	-57.4	-1.88	
DJPP-20	-8.92	-115.0	-14.32	
DJPP-21	-8.96	-116.3	-14.45	
WYDAK-22	-7.00	-118.1	-13.92	
WYDAK-23	-12.18	-106.1	-11.91	
WYDAK-24	-14.23	-105.3	-11.58	
WYDAK-25	-13.33	-119.4	-13.86	
LR-27	-4.37	-33.8	0.65	
LR-28	-13.54	-70.7	-7.00	
LR-29	-16.77	-63.8	-5.03	
LR-30	-9.44	-58.2	-2.77	
LC-31	0.40	-39.9	1.91	0.71714
JBPP-32	-5.19	-97.1	9.15	

Stable Isotope Ratios (2/2)				
Sample ID	δ13C (ratio)	δD (ratio)	δ18O (ratio)	Sr (87/86) (ratio)
WA-33		-60.8	-5.46	0.71163
WA-34		-53.9	-4.36	0.71161
WA-35		-42.9	-1.43	0.71429
WA-36		-39.2	-0.49	0.72264
WA-37		-46.9	-3.97	High Ba
WA-38		-56.0	-5.95	0.7099
WA-39		-42.2	-3.25	0.71494
WA-40		-45.1	-2.06	0.71167
LB-42		42.1	-6.33	0.72019
LB-43		-94.7	-9.44	0.70842
LB-44		-103.6	-10.68	0.70911
LB-45		-52.9	-2.81	0.70865
LB-46		-57.7	-2.60	0.70902
LB-47		-69.8	-4.11	0.70884
LB-48				